Bulgarian Chemical Communications, Volume 50, Issue 2, (pp. 298 –305) 2018

Application of direct simulation Monte Carlo for development of micro gas sensor

M. B. Gerdroodbary*[1], D. D. Ganji[1], M. Taeibi-Rahni[2], Sh. Vakilipour[3], R. Moradi[4]

[1]*Department of Mechanical Engineering, Babol University of Technology, Babol, Iran*
[2]*Department of Aerospace Engineering, Sharif University of Technology, Tehran, Iran*
[3]*Faculty of New Sciences and Technologies, University of Tehran, Tehran, Iran*
[4]*Department of Chemical Engineering, School of Engineering & Applied Science, Khazar University, Baku, Azerbaijan*

Received: November 26, 2017; Revised: January 1, 2018

Development of a new micro gas sensor is essential for the analysis of the outcome of gas separation devices. In this paper, direct simulation Monte Carlo (DSMC) modeling of low-pressure gas sensor was performed to investigate the effect of physical parameters on the performance and main characteristics of this type of actuator in various operating conditions. Extensive parametric studies were done and the effect of ambient pressure, temperature and gap of arms were comprehensively investigated. Our findings showed that gap size significantly influences the flow features and force generation inside the sensor.

Keywords: Knudsen force; DSMC; Rarefied gas; Gas sensor; MEMS.

INTRODUCTION

In recent years, the application of sensors for the detection of gas has become significant due to their importance in industrial devices. Since the first step for the separation of a mixture is detection, the development of this sensor could highly enhance the performance of separation techniques such as membranes, cryogenic column and gas centrifuges [1-3]. In addition, several researchers have tried to develop new simple devices for the detection of dangerous gases such as NH_3, CO and H_2S. There are various techniques to sense the gas component or measure the pressure of the gases. One of the primary goals of the scientists is to develop micro electronic devices for this purpose [4-6].

Since the current sensor for analyzing and sensing of the gas is spacious and expensive, scholars have focused on new methods and devices which are small and simple. The development of the micro-electromechanical system (MEMS) has enabled researchers to decrease the size of the device in micro-scale. Consequently, micro sensors are highly developed due to their applications in different devices such as medical instruments. One of the new methods for gas detection is the application of the Knudsen force which is highly sensitive to the properties of the gas. Indeed, the non-homogeneity of the temperature in low-pressure conditions produces a force known as Knudsen force. Previous studies [7-9] have shown that this type of force is highly sensitive to the pressure of the domain, temperature difference and the type of gas of the domain. These special characteristics motivated the researchers [8] to use this approach for measurement of pressure.

A lot of studies have been devoted to recognize the characteristics of the Knudsen force in rarefied conditions. Ketsdever *et al*. [7] reviewed more than hundred papers and documents to present a comprehensive literature review on the origin of the Knudsen force and its history. Since Crookes radiometer [8] was the first device which applied Knudsen force, various researchers performed extensive studies on this device. Passian *et al*. [9,10] investigated thermal transpiration at the microscale by a Crookes cantilever.

Several works have been performed to apply a direct simulation Monte Carlo (DSMC) for the simulation of a rarefied gas. Poozesh and Mirzaei [11] simulated a fluid flow in a body-fitted grid system using the lattice Boltzmann method. Several similar works also applied this method for solving engineering problems [12-16]. In 2016, Strongrich *et al.* [17, 18] introduced a new device for sensing the pressure by Knudsen force. In this sensor, the hot arm is fixed while the cold arm known as shuttle arm could move and the capacitor is attached to the shuttle arm. Since the gap of these two arms is too small, the Knudsen force acts on the cold side and this could be measured by the capacitor. Fig 1 schematically presents the main mechanisms inside the MIKRA. In our previous work [19], the effect of Knudsen thermal force on the performance of a low-pressure micro gas sensor was completely investigated.

* To whom all correspondence should be sent:
E-mail: mbarzegarg@yahoo.com

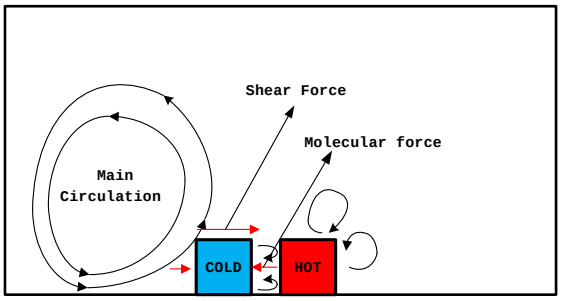

Fig. 1. Scheme of flow inside the MEMS sensor

In the present work, DSMC approach was applied to study the main mechanism of the Knudsen force in rarefied gas condition on the performance of the micro gas sensor (MIKRA). In the first step, the model of the problem is presented and the particle approach is explained. In order to investigate the main technique of this sensor, the flow feature of gas inside the device was thoroughly studied. In addition, the effects of significant parameters such as different ambient pressures, temperature difference of the arms and gap space on the main characteristics of this sensor are presented. Lastly, effective terms on the mechanism of force generation in the low-pressure condition were determined.

NUMERICAL APPROACH

Geometry and assumptions

The generated grid and the boundary condition applied on the model are displayed in Figure 2. According to the size and dimensions of problem, the size of the domain in our work was $600 \times 300\ \mu m$ in x and y direction and 150 by 75 collision cells were generated in the x and y directions, respectively. It was also supposed that the whole surfaces are fully diffuse.

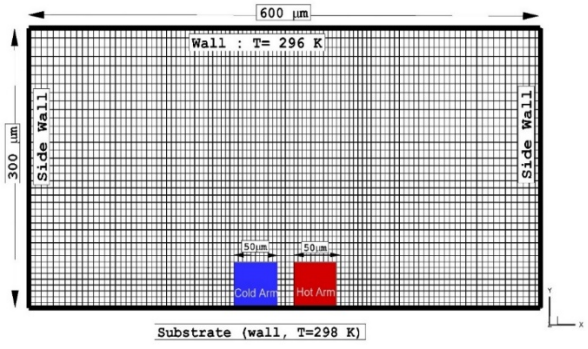

Fig. 2. The boundary conditions and grid of the present model

Governing equations and solver

In order to simulate the low-pressure flow, a conventional numerical method such as CFD was not applied due to assumption of the continuum in the whole domain. In fact, Navier–Stokes equations could not predict the main features of the flow. Thus, Boltzmann equation as a high- order equation should be used and molecular approach is the best approach for such rarefied gas regime. Eq. 1 presents the general formula of the Boltzmann equation:

$$\frac{\partial}{\partial t}(nf) + \mathbf{c}.\frac{\partial}{\partial \mathbf{r}}(nf) + \mathbf{F}.\frac{\partial}{\partial \mathbf{c}}(nf) = Q \qquad (1)$$

where n,$\mathbf{c}$ and f are number density, molecular velocity and velocity distribution function, respectively.

Furthermore,

$$Q = \int_{-\infty}^{+\infty}\int_{0}^{4\pi} n^2(f^* f_1^* - f f_1)\, g\, \sigma\, d\Omega d^3 c_1$$

is the collision integral which defines the variation in the velocity distribution function as a result of intermolecular collisions.

Scientists present various methods for solving the Boltzmann equation. Among various techniques, the DSMC method of Bird [20] is a vigorous and reliable approach for a low-pressure gas flow. In fact, this approach is a particle method based on the kinetic theory for simulation of rarefied gases. Among numerous available DSMC codes, open-source *dsmcfoam* code seems a reliable and professional open code for the simulation of our problem [21]. *dsmcFoam* has been established and presented as toolbox of OpenFOAM version 1.7.

Boundary conditions

In our problem, the whole boundaries of the model were walls with constant temperature. The pressure of the domain varied from 62 pascals to 1500 pascals which induces a Knudsen number from 4.64 to 0.3, respectively. The details of boundary conditions are depicted in fig. 2. The main gas of the domain is nitrogen. As mentioned in the main reference [17], the temperature of the cold and hot arm varied with the pressure of the domain and it is presented in Table 1.

Table 1. Temperature of the cold and hot arm

Pressure	Kn	Hot Arm	Cold Arm
(pa)	-	(K)	(K)
62	4.48	348	304.5
155	1.8	346	304.5
387	0.72	342	304
966	0.29	323	302

Numerical procedure

In order to simulate the collision model in all simulations, the variable hard sphere (VHS) collision model was applied. Since the computational time is related to the number of simulator particles [20], collision pairs were

determined based on the no time counter (NTC) method.

In this study, the gap (distance between the heater and shuttle arms) is known as the length characteristic (L) and it is about 20 microns. The total number of simulated particles was approximately $2.48 \times 10^{+5}$. The space domain was discretized by using squared cells ($\Delta x = \Delta y$), with $\Delta x = 4\ \mu m$, i.e., 150 cells were taken in the x-direction, while the number of cells in the y-direction depends on the aspect ratio *H/W* where *H* and *W* are the width and height of the domain, respectively. It is equal to n_C = 150 × (H/W). The number of particles per cell on the NTC scheme is fixed to 20 and the time step is chosen to be sufficiently smaller (about 1/3) than the cell traversal time, defined as W / ($n_C v_0$) In order to obtain v_0, the $v_0 = \sqrt{2k_B T_0/m}$, with k_B and *m* denote the Boltzmann constant and the gas molecular mass, respectively. According to our calculations, the time step should be less than 3.5×10^{-7}s. We set the time step equal to 1×10^{-8}s, smaller than the mean collision time and close to the time step of the previous works of Strongrich *et al*. [17]. The physical time of these simulations was 0.03 s to reach steady state condition. For a typical simulation, twenty particles were initially set in each cell to minimize the statistical scatter.

RESULTS AND DISCUSSION

Verification

Validation of obtained results is the first step for the simulation studies. In this study, the values of the Knudsen forces on the shuttle arm were compared with experimental data of Strongrich *et al.* [17] at different pressures (fig. 3). The figure also presents the results of SPARTA-DSMC code obtained by Strongrich *et al.* [17]. The comparison confirms that the deviation of obtained data (dsmcfoam) from experimental data is not noticeable and the obtained results are reasonable and reliable for the further studies.

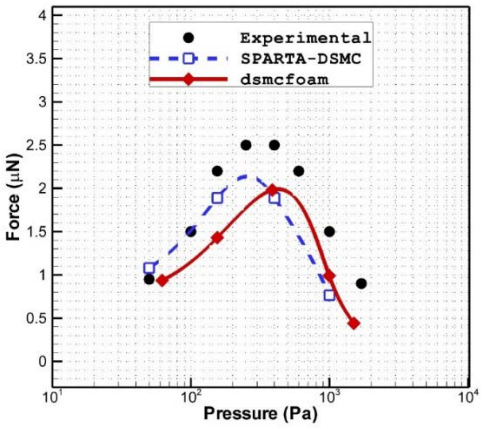

Fig. 3. Comparison of the of obtained results (dsmcfoam) with experimental and numerical data of Strongrich *et al.* [17]

The difference between the numerical and experimental data is due to diverse reasons. The gap distance is the primary reason for this difference.

Flow feature

Figure 4 illustrates the temperature distribution along the streamline patterns for various operating pressures. The figure clearly shows that the circulation is significant at high Knudsen force (P=387 pa). Since the pressure of the domain determines the main characteristics (such as Knudsen number), it is expected that the variation of this term considerably influences the main feature and this is clearly observed in the figure of low-pressure condition (P=62 pa) wherein noticeable kinks in the contour lines are detected.

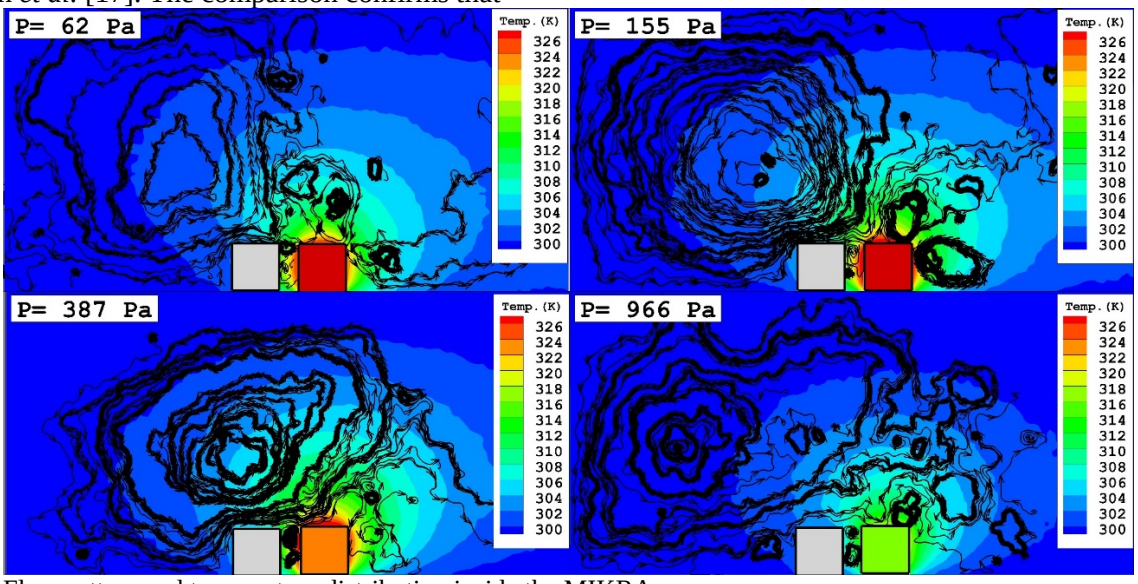

Fig. 4. Flow pattern and temperature distribution inside the MIKRA

As shown in the figure, these kinks originate at the sharp corners on the top of the arms. On the other side, intermolecular collisions rapidly flatten those kinks in the gap of the arms in the high-pressure cases, and the absence of intermolecular collisions allows these kinks to diffuse much further away from the hot arms in the low-pressure conditions as demonstrated in Fig. 4.

In order to reveal the main origin of net force on the shuttle arm, the difference in the pressure on both sides of the cold arm should be investigated. Figure 5 demonstrates the pressure ratio (I) inside the domain for defined pressure conditions. The pressure ratio was calculated as follows:

$$I = \frac{P}{P_{ave}} \qquad (1)$$

where P and P_{ave}denote the local and average pressure of the domain, respectively. According to the contour of the pressure ratio, it is found that the pressure is non-uniformly distributed inside the domain. Indeed, this non-homogeneity of the pressure field is the main reason for an exceptional feature of rarefied gases in our problem. It should be mentioned that non-uniform distribution of temperature does not produce macroscopic streams in the continuum regime, and we do not notice pressure gradients in the absence of external forces. Nevertheless, bulk flows are simply created in a low-pressure condition when there is temperature difference inside the domain. In fact, these streams direct particles in the vicinity of the arms and hereafter make a non-uniform pressure distribution.

Since this is the main driving mechanism for force generation inside Knudsen pumps [22-24], previous studies named this phenomenon as thermal transpiration.

In order to clearly explain the main difference between the various models, the effective terms and mechanism of force generation should be initially explained. As shown in figure 1, thermal gradient in the very low-pressure domain induces a distinctive flow pattern according to pressure and boundary conditions. Thermal stress slip flow (TSS) is the first driven flow in the rarefied domain. This force induces flows from the hot side to the cold side inside the gap of arms. Thermal creep flow is known as the second main force in the low-pressure domain. This type of force, conversely, is produced by the tangential temperature gradient near the wall. The third main force in low-pressure condition is the thermal edge flow and it occurs in sharp corners. According to these explanations, the large circulation of the domain is due to thermal stress slip flow and the thermal edge flow occurs on the right side of the hot arm in the vicinity of the edge. Since thermal stress slip flow which induces a hot to cold flow produces the measurable Knudsen force on the shuttle arm, this study greatly focuses on this type of force.

Thermally driven flow is the main cause for the generation of the Knudsen force. Hence, the analysis of temperature distribution inside the domain is significant. Figure 4 clearly depicts that the temperature gradient is dominant at the high Knudsen number. Indeed, rarefied gas allows molecules to transmit the temperature of hot arm to the domain. As the pressure of the domain is increased, the intermolecular reaction reduces the temperature gradient inside the domain. One of the main significant aspects of the high temperature gradient inside the domain is the pressure difference. Figure 5 clearly confirms that the pressure difference is significant in rarefied

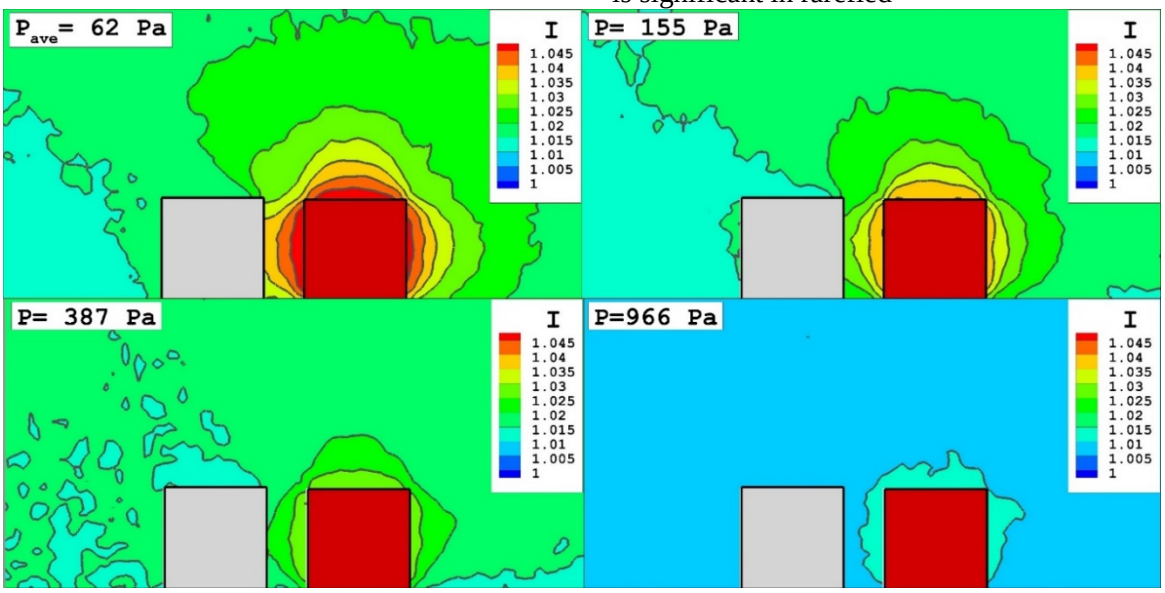

Fig. 5. The distribution of the pressure ratio inside the MIKRA

conditions. Indeed, the temperature gradient induces the pressure difference on the two sides of the cold arm. Our simulation shows that the value of the shear stress on the top of the cold arm is small and is about 1% of the molecular force on the two sides of the cold arm.

In order to investigate the influence of the pressure and temperature distribution on the force production inside the MIKRA, the force distribution of the two sides of the cold arm is plotted in figure 6. The plot clearly shows that the variation of the force on the left side of the cold arm is constant while the force distribution on the right side of the cold arm varies along the height of the arm. The variation of the force confirms that the force production inside the MIKRA is due to the pressure gradient induced by temperature distribution.

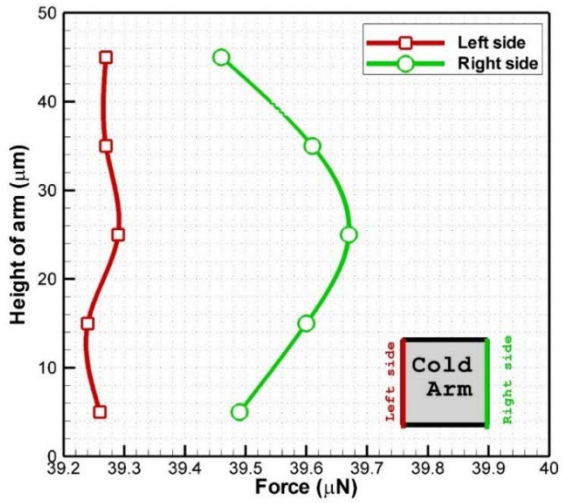

Fig. 6. Comparison of the force distribution on two sides of the cold arm at P=387 pa

Effect of gap distance

Figure 7a compares the temperature distribution and streamline patterns inside the domain for different gap sizes at a specific pressure (P=387 pa) with a similar temperature difference. The contour clearly shows that the flow pattern becomes uniform and the main circulation is strengthened in the low gap size. Since the temperature inside the gap is not significantly varied and the vortex is limited by the gap size, no vortex is formed inside the gap. On the top of the arm, the relatively large space along the thermal creeping flow (cold to hot) permits a big vortex to be formed and the pressure driven flow effectively takes away some molecules from the top wall of the arms and thus releases some pressure therein. In fact, the non-uniform pressure along with large space intensifies the formation of Poiseuille flows and hence a large vortex is formed on the top of the arms.

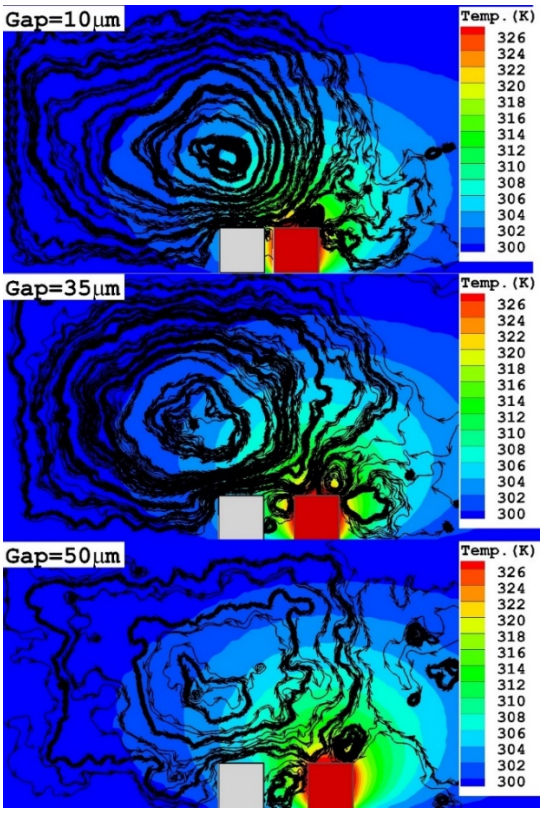

a)

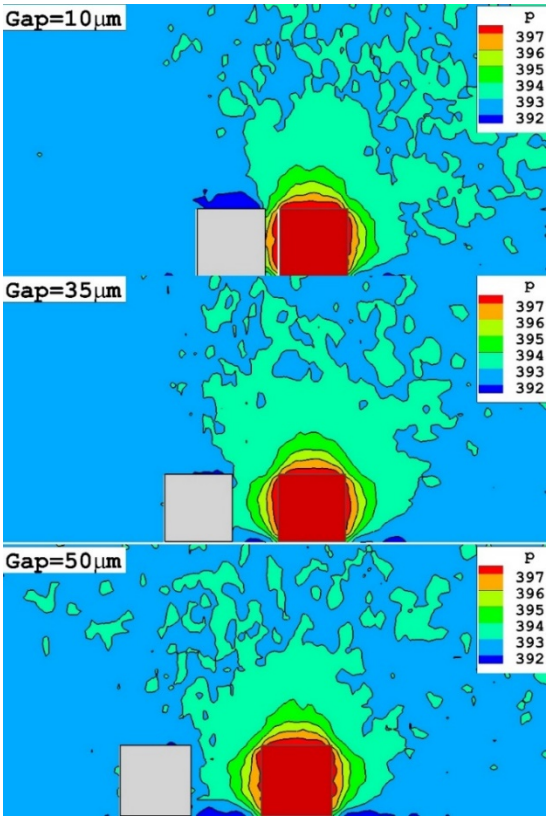

b)

Fig. 7. Effects of gap on a) temperature and streamline b) pressure distribution inside the domain at P=387 pa

As the gap size is increased (Gap=35 μm), the Knudsen number decreases. Hence, the non-uniformdistribution of temperature inside the gap only induces a non-uniform density gradient in the whole domain and pressure gradient diminishes on the top of arm [23]. This distance also declines the strength of thermal creeping flow. Figure 7b compares the pressure distribution for different gap sizes. Hence, the formation of the main vortex deteriorates when the gap size is increased. In addition, a small vortex is generated in the right and top side of the hot arm. This confirms that the pressure driven flow on the top of the arms was limited in the low Knudsen number. In the space of the arms, two vortexes are produced in the space due to non-uniform temperature distribution. In the followings, the effect of these vortices on the force generation on the cold arm will be comprehensively discussed.

In the high gap distance (Gap=50 μm), the pressure gradient becomes less and the formation of the small vortex close to the hot arm does not allow the main counterclockwise vortex to sense the temperature gradient and the clockwise small vortex further blocks the gas molecules flowing out of the gap. In addition, the pressure near the bottom of the gap is lower than the pressure on the top of the arms and this produces a big vortex inside the gap.

Since the main goal of this device (MIKRA) is to measure the force in various pressure conditions, the comparison of the force for the different gap sizes is significant. Figure 8 compares a generated force for different pressures and gap sizes..

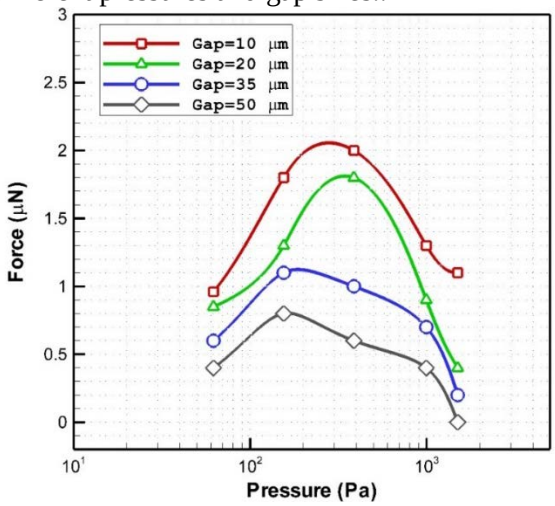

Fig. 8. Influence of the gap distance on the force production on the cold arm

The plot clearly shows that the Knudsen force increases when the gap size is decreased. In addition, it was found that the maximum force occurs at low pressure as the gap size is increased. Indeed, the presence of the vortex diminishes the force production on the right side of the cold arm and does not allow the hot molecules to reach the surface of the cold arm

Effect of arm length (L)

In order to characterize the main mechanism of the operation of MIKRA, the length of the arms is varied to reveal the effect of this factor on the flow feature and Knudsen force generation on the actuator arm. Figure 9 compares the flow features inside the domain for three different values of length when thickness (50 μm) and pressure (P=387 pa) of the model remain constant. The contour shows that increasing the length of the arms divides the main circulations into two circulations.

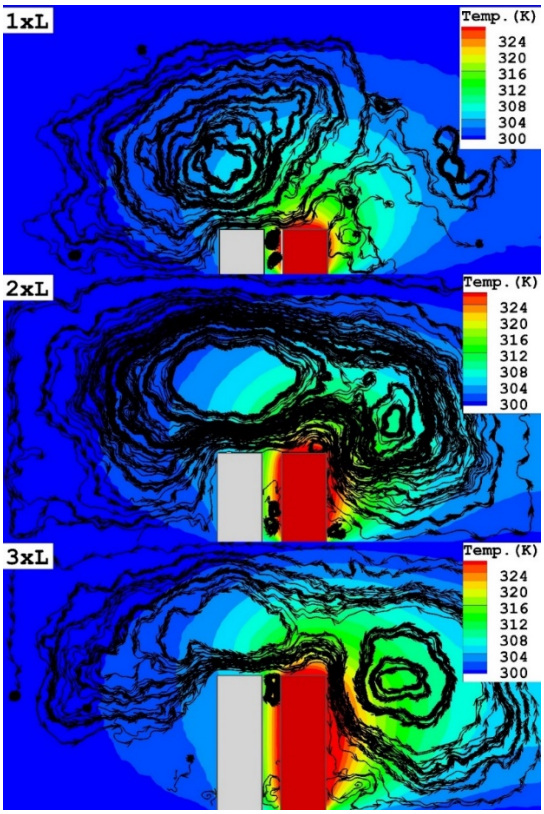

Fig. 9. Effect of the arm length (L) on flow pattern and temperature distribution inside the gas sensor (P=387 pa)

Moreover, the temperature gradient inside the domain significantly intensifies by increasing the length of arms. Figure 10 illustrates the variation of the force generation on the cold arm with various length values at various domain pressures. The induced Knudsen force noticeably increases as the length of the arms is raised. The value of maximum Knudsen force increases 366 percent by rising the length of arm from 1×L to 3×L. This shows that the rate of the induced force on the arms is more than the elongation rate. In addition, the maximum force is obtained at the same pressure for all arm lengths.

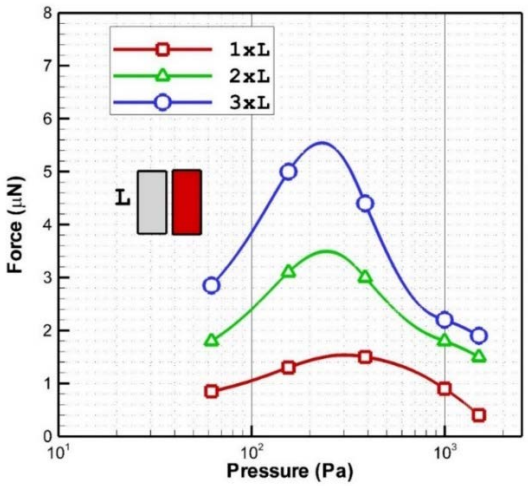

Fig. 10. Effect of the arm length on the Knudsen force generation

CONCLUSIONS

In this research, DSMC method was applied to simulate rarefied gas inside the MEMS device. This work focuses on the influence of ambient pressure on the flow features and force generation mechanism. The governing equation of the current problem is Boltzmann equation. DSMC approach was then applied to simulate the rarefied gas. The flow patterns and temperature distribution were compared for various values of pressure and gap size. Results showed that the gap size considerably influences the generated force, and the maximum force varied by the gap size. Our findings confirmed that the Knudsen force decreases when the pressure of the domain increases. Finally, the force distribution on the right side of the cold arm clearly confirms that the temperature gradient in the gap is significant for the force generation and plays a crucial role in the performance of this device.

REFERENCES

1. C. Liu, Ch.-Sh. Liu, X. Yan, *Physics Letters A*, **381**(12),1092 (2017)
2. A. Peyghan, F. R. Somayeh, L. N. Hadipour, *Phys. Lett. A* **378** (30), 2184 (2014).
3. S. K. Dadzie, J. M. Reese, *Phys. Lett. A* **376**, 967 (2012).
4. A. Hassanvand, M. B. Gerdroodbary, R. Moradi, Y. Amini. *Res. in Phys*. **9**, 351 (2018).
5. T. Goto, T. Itoh, T. Akamatsu, N. Izu, W. Shin, *Sens. and Actuat. B*: *Chemical*, **223,** 774 (2016).
6. G. Gregis, J.-B. Sanchez, I. Bezverkhyy, G. Weber, F. Berger, V. Fierro, J.-P. Bellat, A. Celzard, *Sensors and Actuators B: Chemical*, **vol.** 391 (2017).
7. A. Ketsdever, N. Gimelshein, S. Gimelshein, N. Selden, *Vacuum*, **86**, 1644 (2012).
8. W. Crookes, *Philos. Trans. R. Soc. London*, **164**, 501 (1874).
9. A. Passian, R. Warmack, T. Ferrell, T. Thundat, *Phys. Rev. Lett*. **90**, 124503 (2003).
10. A. Passian, A. Wig, F. Meriaudeau, T. L. Ferrell, T. Thundat, *J. Appl. Phys*., **92**, 10 (2002)
11. A. Poozesh, M. Mirzaei, *J. Stat. Phys.* **166**, 354 (2017).
12. M. Barzegar Gerdroodbary, D. D. Ganji, I. Shiryanpour, R. Moradi. *J Nat Gas Sci Eng*., **53,** 317 (2018):
13. M. B. Gerdroodbary, M. Mosavat, D.D. Ganji, M. Taeibi-Rahni, R. Moradi, *Vacuum*, **150**, 207 (2018)
14. M. B. Gerdroodbary, A. Anazadehseyd, A. Hassanvand, R. Moradi, *Int. J. Hydrog. Energy*, **43** (11), 5770 (2018)
15. M. B. Gerdroodbary, D. D. Ganji, M. Taeibi-Rahni, Shidvash Vakilipour, *Microsystem Technologies*, **24** (5)**.**, 2189 (2018),
16. A. Mahyari, M. Barzegar Gerdroodbary, M. Mosavat, D. D. Ganji. *Cas. Stud. in Therm. Eng*. **12**, 276, (2018).
17. A. D. Strongrich, A. J. Pikus, I. B. Sebastiao, D. Peroulis, A. A. Alexeenko, *IEEE 29th Int. Conf. on Micro Electro Mechanical Systems (MEMS)* (IEEE, 2016), p. 828.
18. A. Strongrich, A. Alexeenko, *Applied Physics Letters*, **107**, 193508 (2015).
19. M.B. Gerdroodbary, D.D. Ganji, M. Taeibi-Rahni, S. Vakilipour, *Europ. Phys. J. Plus*, **132** (7), 315 (2017)
20. G.A.Bird, *Oxford*, *Clarendon Press*; 1994.
21. OpenFOAM: the Open Source CFD Toolbox, User Guide, Version 1.6, (2009).
22. T. Zhu, W. Ye, *Physical Review* E, **82**, 036308 (2010).
23. S. McNamara, Y. B. Gianchandani, *J. Microelectromech. Syst*. **14**, 741 (2005).
24. T. Zhu, W. Ye, J. Zhang, *Physical Review* E, **84**, 056316 (2011).

ПРИЛОЖЕНИЕ НА ДИРЕКТНА МОНТЕ КАРЛО СИМУЛАЦИЯ ЗА РАЗРАБОТВАНЕ НА МИКРО ГАЗОВ СЕНЗОР

М.Б. Гердроодбари*[1], Д.Д. Ганджи[1], М. Таеиби-Рахни[2], Ш. Вакилипур[3], Р. Моради[4]

[1] *Департамент по механоинженерство, Технологически университет на Бабол, Бабол, Иран*
[2] *Департамент по космическо инженерство, Шариф Технологичен университет, Техеран, Иран*
[3] *Факултет по нови науки и технологии, Техерански Технологичен университет, Техеран, Иран*
[4] *Катедра по химическо инженерство, Училище по инженерство и приложна наука, Казарския университет, Баку, Азербайджан*

Постъпила на 26 ноември 2017 г.; коригирана на1 януари 2018 г.

(Резюме)

Разработването на нов микро газов сензор е съществено за анализа на излизащите газове от газоразделителни устройства. В настоящата статия е моделиран газов сензор за ниско налягане чрез директна Монте Карло симулация с цел изследване на влиянието на физичните параметри върху работата и основните характеристики на този вид устройства при различни условия на работа. Проведено е задълбочено параметрично изследване върху влиянието на атмосферното налягане, температурата и разстоянието между рамената на устройството. Установено е, че разстоянието има значително влияние върху характеристиките на потока и генерацията на сила в сензора.